A topologically unique alternating $\{Co^{III}_3Gd^{III}_3\}$ magnetocaloric ring

María José Heras Ojea,[a] Giulia Lorusso,[b] Gavin A. Craig,[a,c] Claire Wilson,[a] Marco Evangelisti,[b]* and Mark Murrie[a]*

[a]WestCHEM, School of Chemistry, University of Glasgow, University Avenue, Glasgow, G12 8QQ, UK

[b]Instituto de Ciencia de Materiales de Aragón (ICMA), CSIC and Universidad de Zaragoza, 50009 Zaragoza, Spain.

[c]Institute for Integrated Cell-Material Science (WPI-iCeMS), Kyoto University, Yoshida, Sakyo-ku, Kyoto 606-8501, Japan (current affiliation).

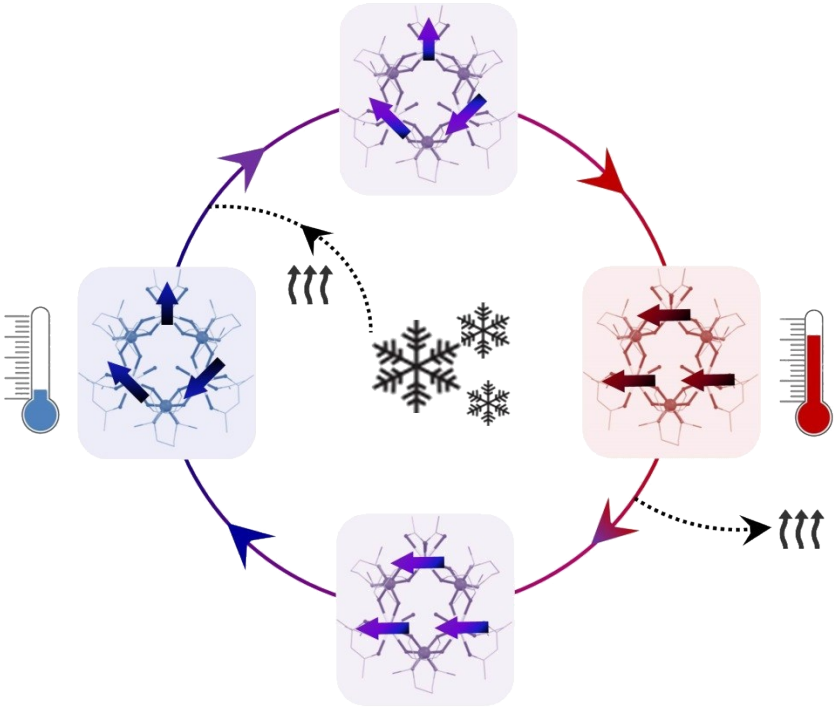

Contents

Experimental section

Materials and physical measurements

All reagents and solvents were obtained from commercial suppliers and used without further purification. The polydentate ligand H_6L used in the synthetic routes is the commercial reagent 2,2'-(propane-1,3-diyldiimino)bis[2-(hydroxymethyl)propane-1,3-diol] (H_6L).

The IR spectra were measured using a FTIR-8400S SHIMADZU IR spectrophotometer. The microanalyses and mass spectroscopic studies were performed by the analytical services of the School of Chemistry at the University of Glasgow. The UV-Vis spectrum of **1** was measured in a Shimadzu UV-1800 UV spectrophotometer.

Synthetic methods

$[Co(H_6L)(CH_3COO)_2]$ (**1**): $Co(CH_3COO)_2{\cdot}4H_2O$ (4.98 g, 20 mmol) was added to a white suspension of H_6L (5.64 g, 20 mmol) in isopropanol (100 mL), resulting in a pale pink suspension. The pink suspension was stirred overnight at room temperature. Yield 75% (6.90 g). IR: $\bar{\upsilon}$ (cm^{-1}) = 3198, 2874, 1560, 1406, 1269, 1034, 1013, 768, 660. Elemental analysis ($[Co(H_6L)(CH_3COO)_2]$) [%], found: C 39.25, H 7.08, N 6.06; calc: C 39.22, H 7.02, N 6.10. MS (ESI+, m/z): 362 $Na[Co(H_4L)]^+$, 340 $[Co(H_5L)]^+$.

$[Co^{III}_3Gd^{III}_3(H_2L)_3(acac)_2(CH_3COO)_4(H_2O)_2]$ (**2**): $Gd(acac)_3{\cdot}H_2O$ (0.10 g, 0.21 mmol) was added to a pink suspension of $[Co(H_6L)(CH_3COO)_2]$ (0.10 g, 0.21 mmol) in a mixture of $4CH_3CN$:$1CH_3OH$ (20 mL), turning the pink suspension into a purple solution. The final solution was stirred and heated to 85°C for 45 min. Dark purple block-like single crystals suitable for X-ray diffraction were obtained by slow diffusion of tetrahydrofuran into the solution over one week. Yield 20% (26 mg). IR: $\bar{\upsilon}$ (cm^{-1}) = 2971, 1576, 1520, 1449, 1366, 1217, 1036, 685. Elemental analysis ($[Co_3Gd_3(H_2L)_3(acac)_2(CH_3COO)_4{-}(H_2O)_2]{\cdot}0.5CH_3OH{\cdot}4H_2O$) [%], found: C 30.24, H 5.04, N 3.92; calc: C 30.29, H 5.23, N 4.12.

Spectroscopic studies

Fig S1 IR spectra for $[Co(H_6L)(CH_3COO)_2]$ (**1**) and $[Ni(H_6L)(CH_3COO)_2]$. The inset shows the crystal structure of $[Ni(H_6L)(CH_3COO)_2]$.

The position of the frequency bands related to the acetate groups in the spectrum of **1** ($\upsilon_{(C=O)}$ = 1561 cm^{-1}, $\upsilon_{(C-O)}$ = 1406 cm^{-1}) suggests that the counterions are coordinated to the Co(II) ions in a monodentate mode.[1, 2] The similarity between both spectra, the tendency of H_6L to encapsulate 3*d* metal ions in the central $\{N_2O_2\}$-pocket previously shown by other complexes,[3-5] and given that the crystal structure of $[Ni(H_6L)(CH_3COO)_2]$ is known,[6] we believe that the Co(II) ion in **1** presents an analogous coordination environment to that displayed for the nickel monomer.

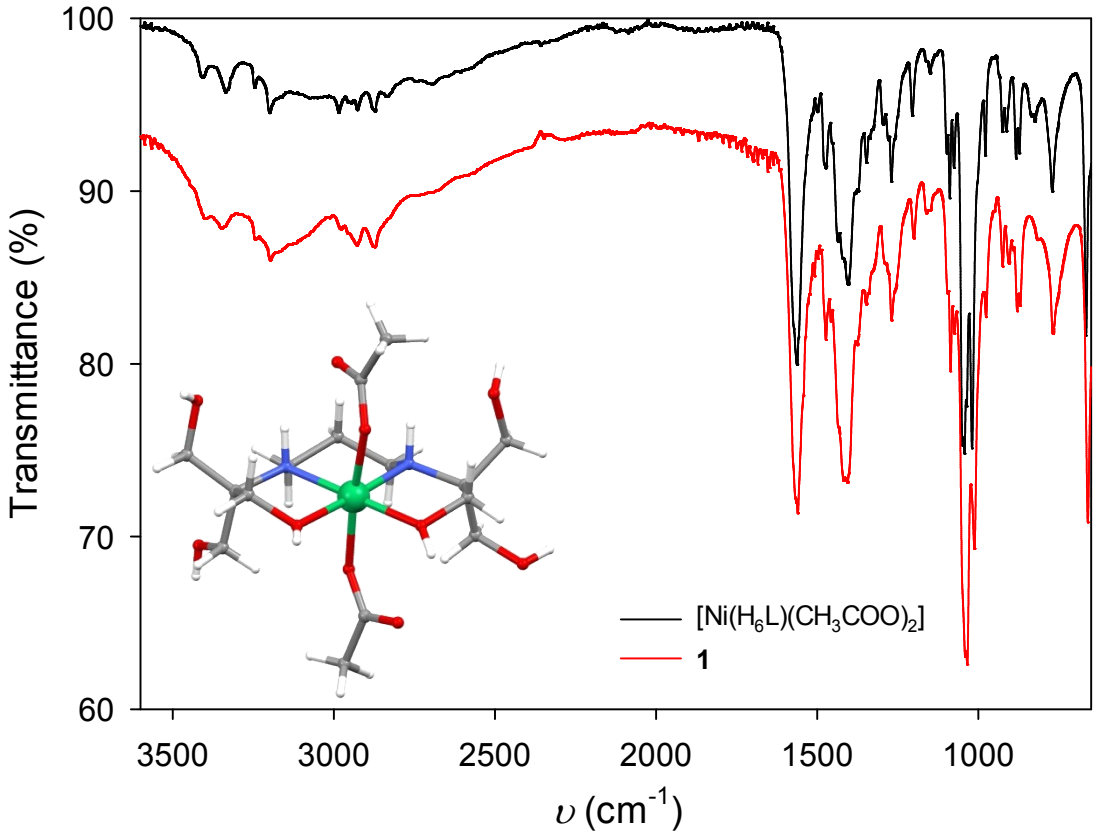

Fig S2 UV-Vis spectrum for **1**. The studies were performed on methanolic solutions of **1** at *c* = 1 mM, 5 mM, 50 mM.

The spectra corresponding to $^{c}_{2}$ = 5 mM and $^{c}_{3}$ = 50 mM display three broad absorption bands around λ = 495, 520, 565 nm. The most diluted solution $^{c}_{1}$ = 1 mM shows only the band around 520 nm.

By applying the Beer-Lambert law ($A = \varepsilon \cdot l \cdot c$) we are able to calculate the molar absorption coefficient (ε) of the displayed bands at different concentrations, giving $^{\varepsilon}_{495}$ = 17 ($^{c}_{2}$), 20 ($^{c}_{3}$) L·mol^{-1}·cm^{-1}, $^{\varepsilon}_{520}$ = 16 ($^{c}_{2}$), 19 (c_3) L·mol^{-1}·cm^{-1}, $^{\varepsilon}_{565}$ = 23 (c_1), 15 ($^{c}_{2}$), 17 ($^{c}_{3}$) L·mol^{-1}·cm^{-1}. Considering that all the values are comprised in the range of 10 – 100 L·mol^{-1}·cm^{-1}, the bands are related to the spin-allowed *d-d* transitions for octahedral Co(II) complexes.

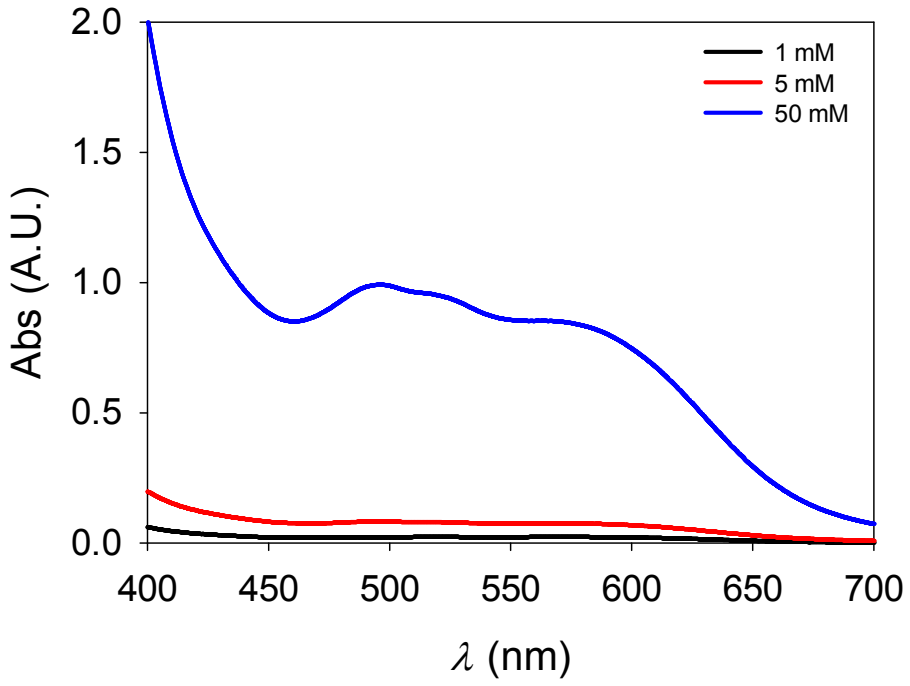

The crystal field parameter Δ_0 = 9588 cm^{-1}, and the Racah parameter B = 827 cm^{-1}, have been calculated taking into account that:

λ ~ 565 nm: $^{\upsilon}_{1}$ = 17746 cm^{-1}, related to $^4A_{2g} \leftarrow {}^4T_{1g}$

λ ~ 520 nm: $^{\upsilon}_{2}$ = 19305 cm^{-1}, related to $^4T_{1g}(P) \leftarrow {}^4T_{1g}$

λ ~ 495 nm: $^{\upsilon}_{3}$ = 20177 cm^{-1}, related to spin-orbit coupling effects.

The observed absorption bands were assigned according to previous studies on octahedral $[Co^{II}(H_2O)_6]^{2+}$ complexes.[7] The extracted crystal-field splitting value ($\Delta_0/B \approx 12$), is consistent

with high-spin Co(II) in **1**, in good agreement with the results of the dc magnetic experiments performed on **1** (see Fig S10).

Therefore, the conclusions extracted from the UV-Vis spectroscopy are consistent with the ligand-metal arrangement previously proposed, *i.e.* $[Co(H_6L)(CH_3COO)_2]$ (see IR discussion), and with those from the rest of characterisation techniques.

Fig S3 ESI^+ mass spectrum for **1**. The experiments were carried out using methanol as a solvent.

The majority of the displayed peaks were assigned considering results from the IR, the molecular weight and the charge of the potential cations which could be present in solution after some fragmentation processes. The spectrum for complex **1** shows peaks related to a monomeric species ($[Co(H_5L)]^+$, $[Co(H_4L)]Na^+$). The monodentate acetate anions could have been removed from the structure due to the relatively high lability of the Co-O(CH_3CO) bonds compared to the $\{N_2\text{-}O_2\}$ ones from the chelating ligand. Furthermore, the peaks observed in the region of 150-310 g/mol suggest a possible fragmentation of some hydroxyl groups from H_6L chelating ligand (*e.g.* $[Co(H_5L)\text{-}2(OH)]^+$).

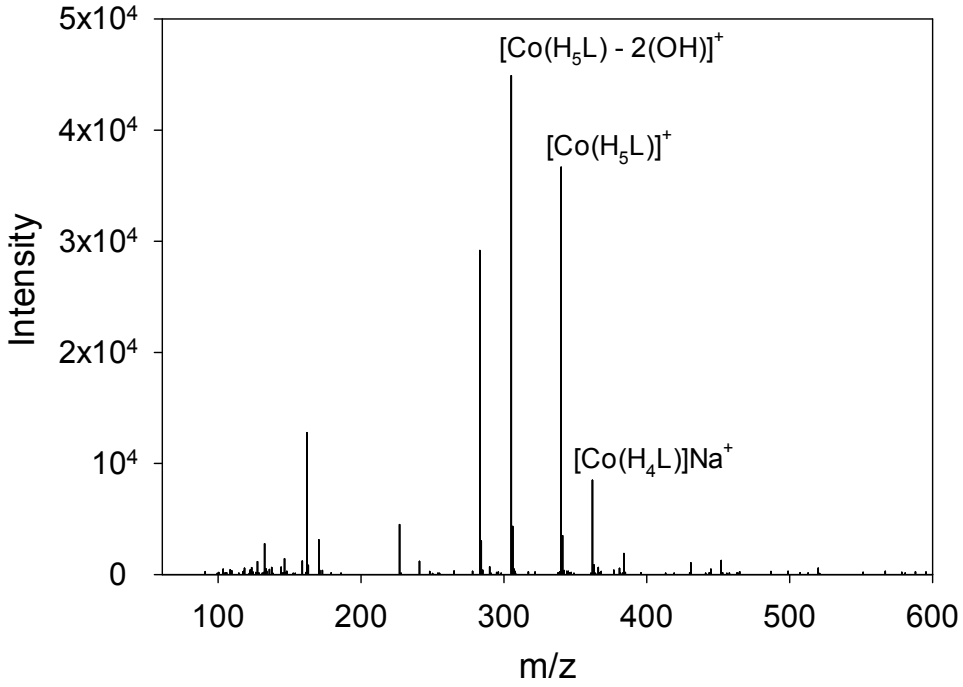

Crystallographic details

Crystallographic data was collected for **2** at 100 K using Mo-Kα radiation (λ = 0.71073 Å), using a Bruker-Nonius Kappa CCD diffractometer with an Oxford Cryosystems cryostream device mounted on a sealed tube generator. The structure was solved using SUPERFLIP[8] and refined using full-matrix least squares refinement on F^2 using SHELX2014[9, 10] within OLEX2.[11]

Complex **2** crystallises in the tetragonal space group *I*-42*d* (see Table S1). The asymmetric unit contains 1/2 molecule of $[Co^{III}_3Gd^{III}_3(H_2L)_3(acac)_2(CH_3COO)_4(H_2O)_2]$. The structure contains also significant solvent accessible voids. Difference Fourier maps of the solvent regions suggest the presence of several CH_3CN, CH_3OH, and H_2O molecules in the crystal lattice. However, they are poorly defined, and it was not possible to obtain a good model. Consequently, SQUEEZE (in PLATON)[12, 13] was used to identify the solvent voids and account for the electron density within them, calculated to contain 2124 electrons per unit cell, corresponding to approximately 265 electrons per complex.

The central carbon atom of one of the H_2L^{4-} ligand units (C201) was modelled over 2 half occupied positions related by a 2-fold rotation and together with one of the terminal carbon sites of the $acac^-$ group (C5A) it was refined with an isotropic adps. Hydrogen atoms were placed in geometrically calculated positions and refined as part of a riding model except OH^-, H_2O, CH_3COO^- and $acac^-$ (H1AA, H1AB, H1AC, H5AA, H5AB, H5AC) hydrogens which were refined as part of a rigid rotating group.

Fig S4 Detail of the metal alkoxide core of **2**. Co, fuchsia; Gd, green; N, blue; O, red. Polyhedra are shown in fuchsia (Co) and green (Gd).

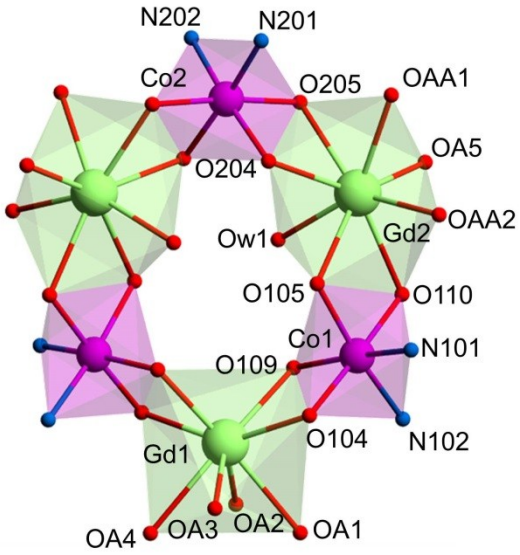

Fig S5 Planes defined by the different metal ions in **2**. Co, fuchsia; Gd, green; N, blue; O, red.

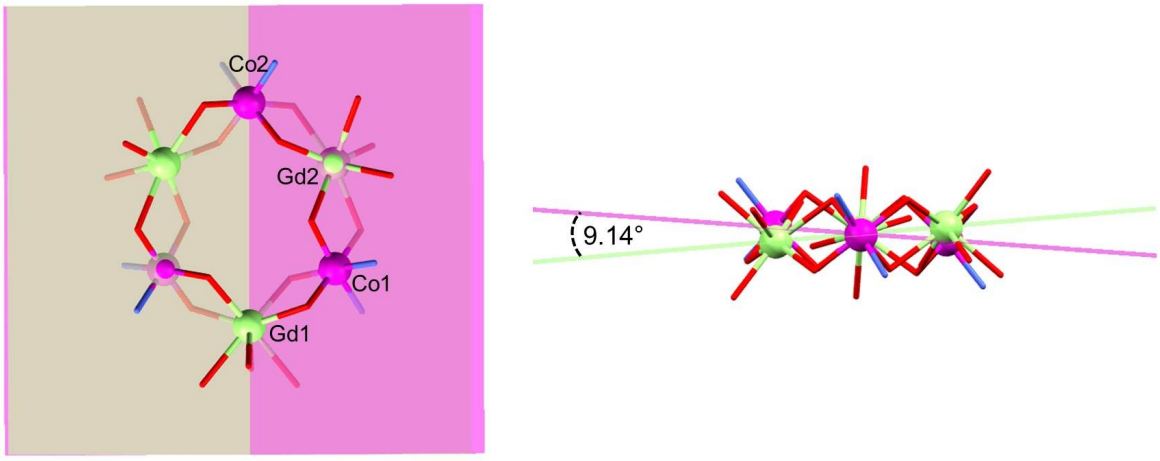

Table S1 Crystal Data and Structure Refinement Parameters of **2**.

Complex	**2**
T/K	100(2)
Crystal system	tetragonal
Space group	*I*-42*d*
a/Å, *c*/Å	26.644(3), 27.368(3)
V/Å^3	19428(4)
Z	8
ρ_{calc}/mg/m^3	1.337
μ/mm^{-1}	2.583
F(000)	7800.0
2θ range for data collection/°	3.678 to 50.118
Index ranges	-31 ≤ *h* ≤ 31, -31 ≤ *k* ≤ 31, -32 ≤ *l* ≤ 32
Reflections collected	246917
Data/restraints/ parameters	8610/590/432
GOF on F^2	1.169
Final *R* indexes [I≥2σ (I)]	R_1 = 0.0353, wR_2 = 0.0838
Final *R* indexes [all data]	R_1 = 0.0490, wR_2 = 0.0967
Largest diff. peak/hole/e Å^{-3}	0.91/-0.66
Flack parameter	-0.013(3)

Table S2 Shape measures of **2**, $\{Co^{III}_3Gd^{III}_3\}$ relative to ideal 8-vertex polyhedra. The lowest CShMs value, and thus most coincident geometry is highlighted in pink.[14, 15] The symmetry analyses around the Gd(III) ion reveal a triangular dodecahedron (D_{2d}) as the closest ideal geometry for both Gd1, and Gd2 centres.

	Gd1	Gd2	Symmetry	Ideal shape
OP-8	36.266	29.523	D_{8h}	Octagon
HPY-8	23.975	23.435	C_{7v}	Heptagonal pyramid
HBPY-8	14.977	16.887	D_{6h}	Hexagonal bipyramid
CU-8	11.482	11.757	*Oh*	Cube
SAPR-8	4.715	2.558	D_{4d}	Square antiprism
TDD-8	**2.895**	**0.990**	$\boldsymbol{D_{2d}}$	**Triangular dodecahedron**
JGBF-8	12.597	13.317	D_{2d}	Johnson gyrobifastigium J26
JETBPY-8	28.056	27.988	D_{3h}	Johnson elongated triangular
JBTPR-8	5.123	2.250	C_{2v}	Biaugmented trigonal prism J50
BTPR-8	4.423	1.689	C_{2v}	Biaugmented trigonal prism
JSD-8	4.968	2.788	D_{2d}	Snub diphenoid J84
TT-8	12.302	12.569	*Td*	Triakis tetrahedron
ETBPY-8	23.595	24.091	D_{3h}	Elongated trigonal bipyramid

Energy-dispersive X-ray (EDX) spectroscopic studies

EDX experiments were carried out using Philips XL 30 Environmental Scanning Electron Microscope (ESEM) at different magnifications. In order to remove complications due to charging, samples were gold-coated using a vacuum electric sputter coater (POLARON SC 7640) prior to analysis. The images were taken using W-K*α* (57981.77 eV) radiation with a Secondary Electron detector and Oxford Instruments INCA 250Xact10 EDX detector.

EDX was performed on a bulk crystalline sample of complex **2**. Multiple, randomly selected, large regions were analysed in order to investigate the homogeneity of the bulk sample (Fig S6−8). The average Co:Gd ratio found for **2** is 3:3 (Avg. Atomic% Co:Gd is 49.7(7):50.3(7)), which is consistent with that established by single-crystal XRD. Further EDX map analyses by using different colour schemes for Co (red) and Gd (green) were performed to establish the distribution of the metal ions in the sample (Fig S9)). These reveal the even distribution of Co/Gd in the crystalline bulk sample.

Fig S6−8 EDX spectra of **2**. The inset displays the area of the sample used for the analysis; the Atomic% is shown for each area.

Region A:

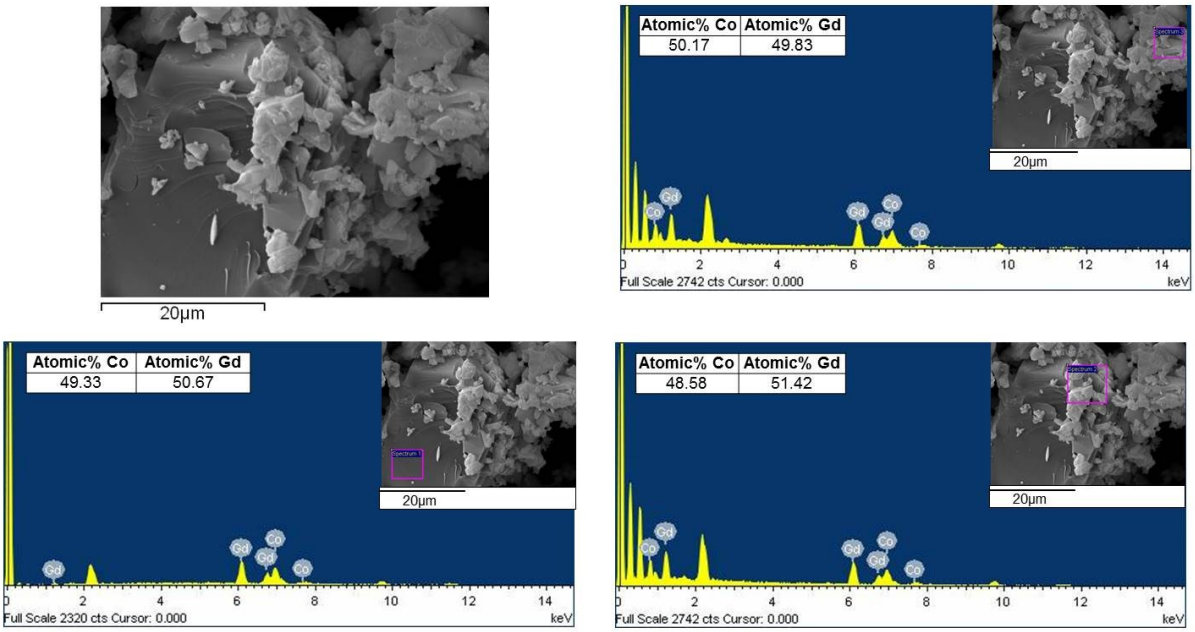

Region B:

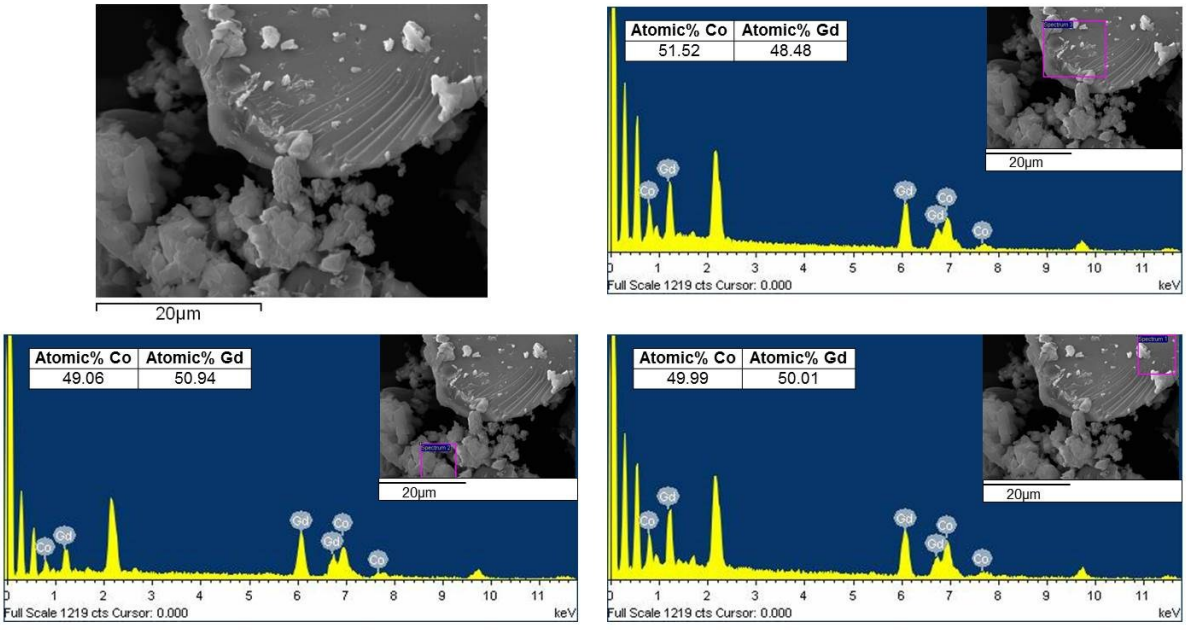

Region C:

Fig S9 EDX elemental map showing the distribution of Co and Gd in a bulk sample of **2** (*regions B and C*). Co is displayed in red, while Gd is in green.

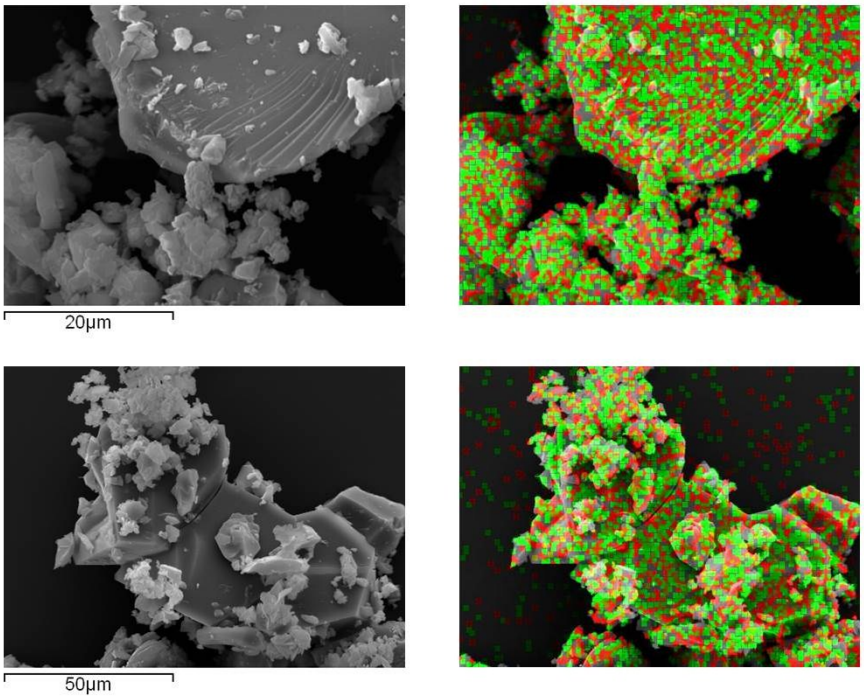

Magnetic and magnetocaloric studies

Magnetic measurements were performed on polycrystalline samples of **1** (in eicosane) and **2** using a Quantum Design MPMS-XL SQUID magnetometer. Data were corrected for the diamagnetic contribution of the sample holder (and eicosane for **1**) by measurements, and for the diamagnetism of the compounds ($\chi_{M_{(dia)}}$ for **2** = $9.78 \cdot 10^{-4}$ $cm^3 \cdot mol^{-1}$).

Heat capacity measurements were carried out for temperatures down to *ca*. 0.3 K by using a Quantum Design 9T-PPMS, equipped with a ^{3}He cryostat. The experiments were performed on thin pressed pellets (*ca*. 1 mg) of a polycrystalline sample, thermalized by *ca*. 0.2 mg of Apiezon N grease, whose contribution was subtracted by using a phenomenological expression.

Fig S10 Temperature dependence of $\chi_M T$ for **1** in an applied field of 1000 Oe.

The room temperature susceptibility value (2.86 $cm^3 \cdot mol^{-1} \cdot K$) is in good agreement with that expected for an anisotropic Co(II) mononuclear complex (2.81 $cm^3 \cdot mol^{-1} \cdot K$, considering S = 3/2, g = 2.45).[16] The experimental values decrease gradually down to 150 K, before reaching a minimum of 1.50 $cm^3 \cdot mol^{-1} \cdot K$ at 2 K. This behaviour is consistent with an octahedral Co(II) centre subject to 1st order spin-orbit coupling.

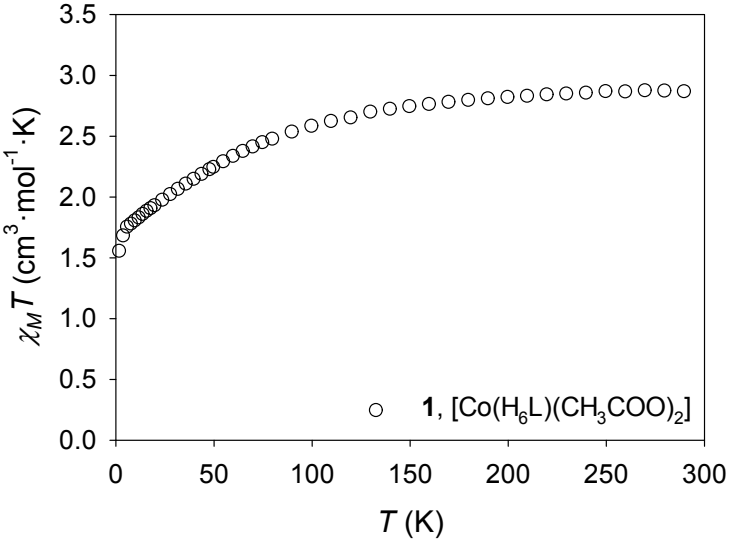

Fig S11 Magnetic model used for the fit of **2**. Co, fuchsia; Gd, green; N, blue; O, red.

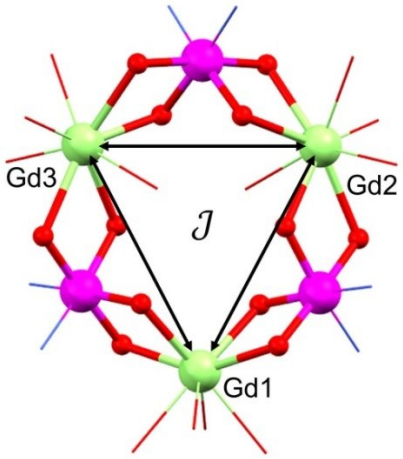

$$\hat{H} = -2J\left(\hat{S}_1 \cdot \hat{S}_2 + \hat{S}_1 \cdot \hat{S}_3 + \hat{S}_2 \cdot \hat{S}_3\right) + g\mu_B \vec{B} \sum_{i=1}^{3} \vec{S}_i$$

Spin Hamiltonian used to fit the magnetic data for **2**, with one parameter J describing the exchange interaction between Gd(III)···Gd(III) centres ($\hat{S}_i$ denotes the spin operator). The second term is the Zeeman interaction, with g as the isotropic single-ion g factor for Gd(III) ion, μ_B the Bohr magneton and $\vec{B}$ the magnetic field.

Fig S12 Intermolecular hydrogen bonding interactions (dashed black lines) in complex **2**. C, grey; Co, fuchsia; Gd, green; H, white; N, blue; O, red All the interactions involve CH_3COO^-···(HO)R hydrogen bonds. The average intermolecular Gd···Gd distance is 10.200(1) Å.

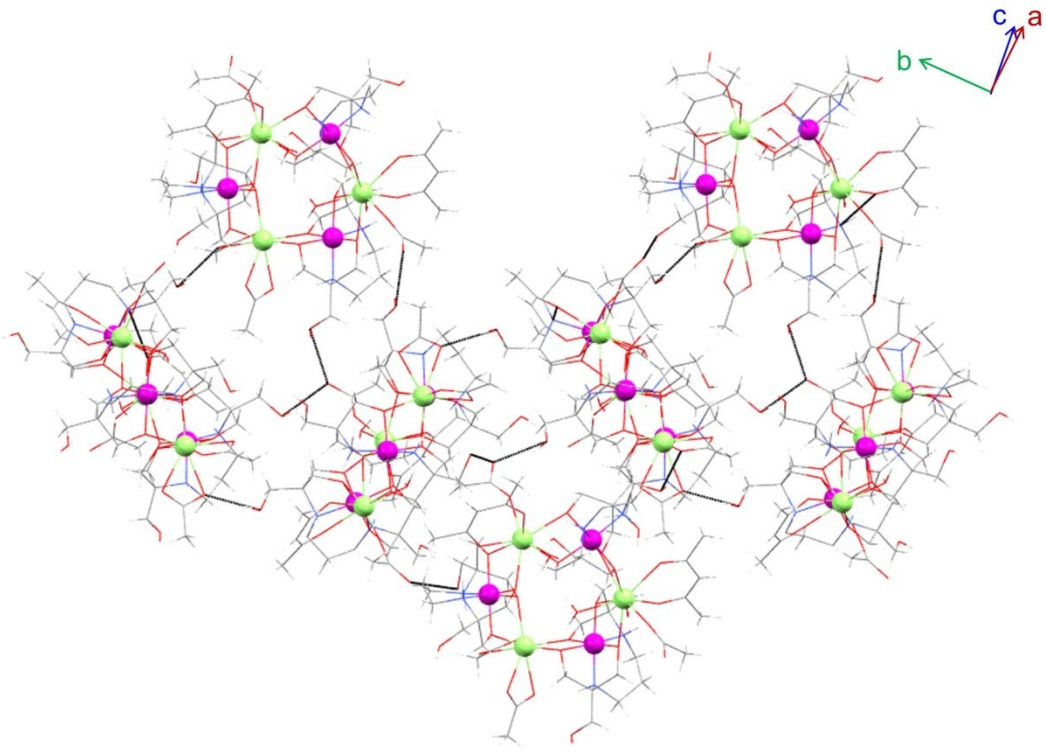

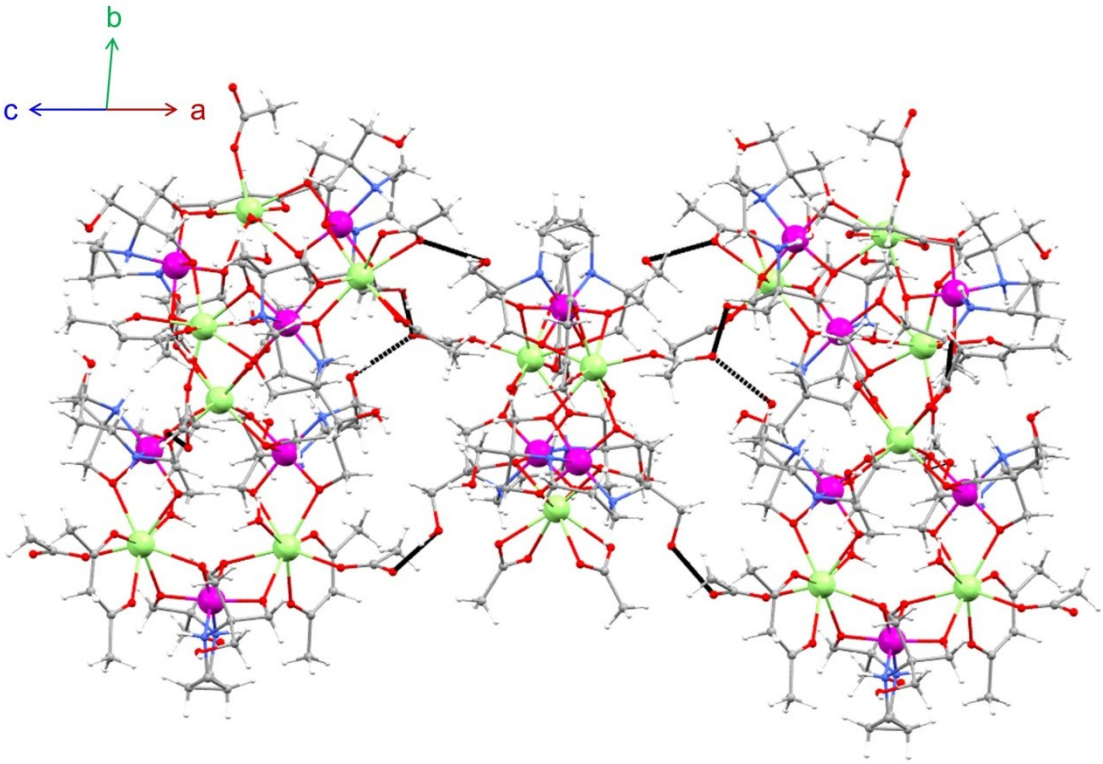

References

1. K. Nakamoto, "*Infrared and Raman Spectra of Inorganic and Coordination Compounds, Part A*" (John Wiley & Sons, Ltd., 1986, 4th edn).
2. G. B. Deacon and R. J. Phillips, *Coordi. Chem. Rev.*, 1980, **33**, 227-250.
3. V. A. Milway, F. Tuna, A. R. Farrell, L. E. Sharp, S. Parsons and M. Murrie, *Angew. Chem. Int. Ed.*, 2013, **52**, 1949-1952.
4. M. Heras Ojea, C. Wilson, S. J. Coles, F. Tuna and M. Murrie, *Dalton Trans.*, 2015, **44**, 19275-19281.
5. M. Heras Ojea, V. A. Milway, G. Velmurugan, L. H. Thomas, S. J. Coles, C. Wilson, W. Wernsdorfer, G. Rajaraman and M. Murrie, *Chem. Eur. J.*, 2016, **22**, 12839-12848.
6. M. Heras Ojea, C. Wilson, M. Murrie, *Unpublished work*.
7. D. R. Armstrong, R. Fortune and P. G. Perkins, *Dalton Trans.*, 1976, 753-757.
8. L. Palatinus and G. Chapuis, *J. Appl. Cryst.*, 2007, **40**, 786-790.
9. G. Sheldrick, *Acta Crystallog. Sect. A*, 2008, **64**, 112-122.
10. G. Sheldrick, *Acta Crystallog. Sect. C*, 2015, **71**, 3-8.
11. O. V. Dolomanov, L. J. Bourhis, R. J. Gildea, J. A. K. Howard and H. Puschmann, *J. Appl. Cryst.*, 2009, **42**, 339-341.
12. P. van der Sluis and A. L. Spek, *Acta Crystallog. Sect. A*, 1990, **46**, 194-201.
13. A. Spek, *J. Appl. Cryst.*, 2003, **36**, 7-13.
14. D. Casanova, M. Llunell, P. Alemany and S. Alvarez, *Chem. Eur. J.*, 2005, **11**, 1479-1494.
15. M. Pinsky and D. Avnir, *Inorg. Chem.*, 1998, **37**, 5575-5582.
16. Y.-Z. Zhang, S. Gomez-Coca, A. J. Brown, M. R. Saber, X. Zhang and K. R. Dunbar, *Chem. Sci.*, 2016, **7**, 6519-6527.